

Nanoscopic properties and application of mix-and-match plasmonic surfaces for microscopic SERS

Virginia Joseph^{1,2}, *Manuel Gensler*³, *Stephan Seifert*^{1,2}, *Ulrich Gernert*⁴, *Jürgen P. Rabe*³,
Janina Kneipp^{1,2*}

Table of Contents

Figure S1: UV/Vis spectra of nanoparticles in solution.

Table S1: Position of plasmon band (λ_{max}), size (from transmission electron microscopy), and particle concentration of the different gold and silver nanoparticles used for immobilization.

Figure S2: SERS spectra of crystal violet on immobilized citrate reduced gold and hydroxylamine reduced silver nanoparticles

Figure S3: SFM images, plasmon spectra and enhancement factor as a function of the concentration of the analyte crystal violet of monodisperse gold nanospheres with a diameter of 15 nm and 30 nm, immobilized with APTES.

Figure S4: SERS spectra of water soluble compounds of different pollen species obtained with gold nanoparticles in solution.

Materials and Methods

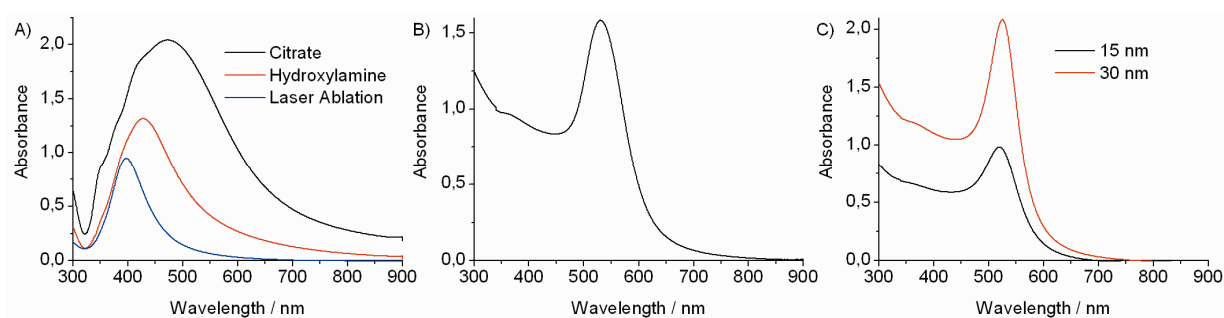


Figure S1: UV/Vis spectra of nanoparticles in solution A) silver nanoparticles prepared by different methods, B) citrate reduced gold nanoparticles prepared according to ref. [1] and C) monodisperse, citrate reduced gold nanoparticles of two different sizes prepared according to ref. [2].

Table S1: Position of plasmon band (λ_{\max})*, size (from transmission electron microscopy), and particle concentration of the different gold and silver nanoparticles used for immobilization.

nanoparticles	λ_{\max} in nm	size in nm	Particle concentration in particles/liter
silver, citrate	475	86 ± 23	$3 \cdot 10^{13}$
silver, hydroxylamine	422	53 ± 22	$1 \cdot 10^{14}$
silver, laser ablation	397	26 ± 11	$9 \cdot 10^{13}$
gold, citrate after ref. ¹	531	29 ± 5	$3 \cdot 10^{14}$
gold, citrate 15 nm after ref. ²	520	15 ± 2	$1 \cdot 10^{15}$
gold, citrate 30 nm after ref. ²	525	30 ± 2	$3 \cdot 10^{14}$

*Please refer to supporting figure S1 for the spectra.

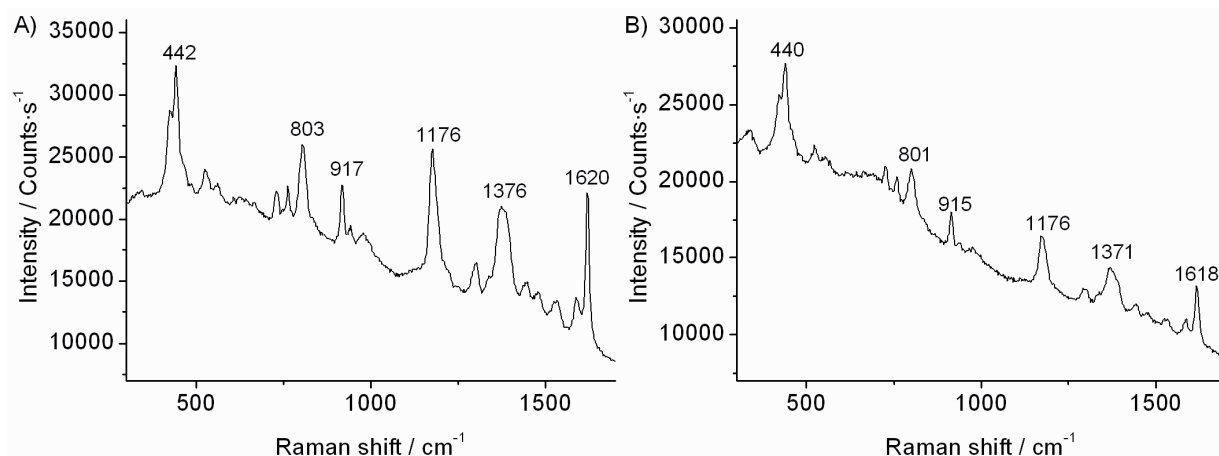


Figure S- 2: SERS spectra of crystal violet on immobilized citrate reduced gold (A) and hydroxylamine reduced silver nanoparticles (B).

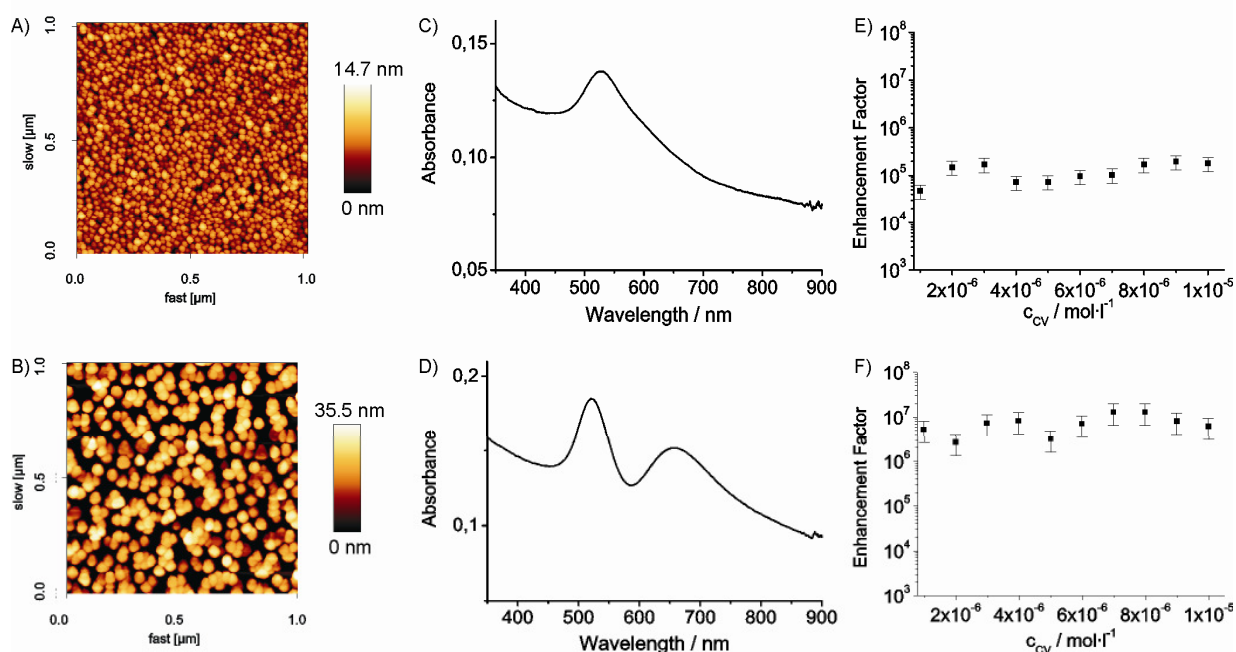


Figure S3: Surface nanostructure (A, B), plasmon spectra (C,D) and enhancement factor as a function of the concentration of the analyte crystal violet (E, F) of monodisperse gold nanoparticles with a diameter of 15 nm (A, C, E) and 30 nm (B, D, F), immobilized with APTES. These citrate-reduced nanoparticles were generated according to the protocol given in ref. ².

The SFM images (A and B) indicate that both types of gold nanoparticles constitute a uniform monolayer with high particle density (see also Table 1). In agreement with the spectra of the Figure 1D, the UV/Vis spectrum of the 30 nm particles has a pronounced second plasmon band, and also the plasmon band of the 15 nm particles on the surface indicates formation of small aggregates on the surface.

We had shown previously that under conditions where no aggregation of the nanoparticles occurs in solution, enhancement is ~10-fold higher for the 30 nm nanoparticles than for the smaller, 15 nm ones, with factors of ~400 as compared to ~40, respectively³. Clearly, the enhancement observed on the surface is much higher for both types of nanoparticles (E and F), which can be ascribed to the favorable conditions caused by the presence of the nanoaggregates in the monolayers (A and B). On the surface, enhancement is ~100 fold higher for the monolayer of the 30 nm nanoparticles compared to the 15 nm nanoparticles (compare E and F). This can be caused by different types of aggregates that can form for different particle sizes^{4,5}.

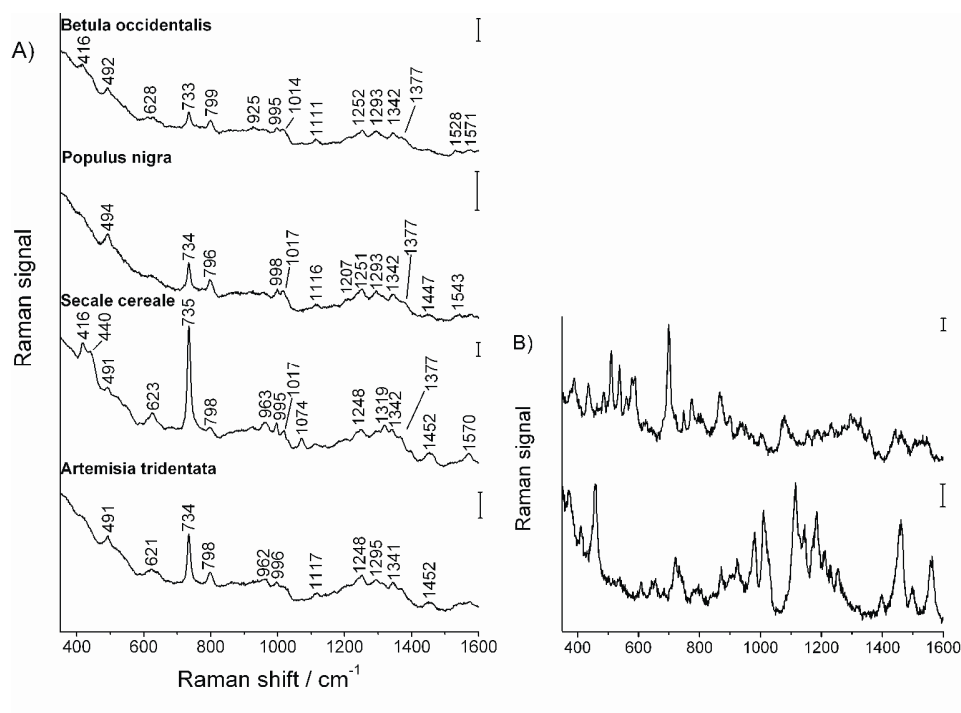


Figure S4: A) Average SERS spectra of aqueous extracts of pollen samples from different plant species and B) exemplary spectra of mixtures of two identically prepared aqueous extracts of pollen from *Artemisia tridentata* obtained with gold nanoparticles in solution, respectively ($\lambda = 785 \text{ nm}$, $I = 6.5 \cdot 10^5 \text{ W} \cdot \text{cm}^{-2}$, acquisition time: 1 s; Raman signal scale bars: A) 50 counts per second, B) 100 counts per second).

Materials and Methods

Preparation of SERS-active surfaces

Gold and silver nanoparticles were synthesized by reduction of 0.0375 mM HAuCl_4 solution (Sigma-Aldrich) and 1.16 mM silver nitrate solution (AgNO_3 , Sigma-Aldrich) with 1 % sodium citrate solution (Chemsolute) according to the procedure described by Lee and Meisel¹. Monodisperse gold nanoparticles were synthesized by seed-mediated growth with sodium citrate according to the method described in ref.². Silver nanoparticles were also synthesized by reduction of AgNO_3 with hydroxylamine hydrochloride (Sigma Aldrich) by rapid addition of a hydroxylamine hydrochloride/sodium hydroxide solution (15 mM / 30 mM, respectively) to a 1 mM silver nitrate solution according to ref.⁶. Additionally to chemical preparation, silver nanoparticles were generated using laser ablation⁷ by irradiation of a silver foil in water with a Nd:YAG laser ($\lambda = 1064$ nm, $\nu = 10$ Hz, 16.6 mJ / pulse) for 10 minutes.

The nanoparticles were immobilized on glass slides using 3-aminopropyltrimethoxysilane (APTMS, 97 %, Sigma) and 3-aminopropyltriethoxysilane (APTES, 98 %) according to methods described in detail in refs.⁸⁻¹¹. Prior to the functionalization with silane, the glass slides were cleaned with a mixture of hydrogen peroxide and sulfuric acid (4:1, v/v). The clean substrates were then immersed for 30 minutes in a solution of methanol (in case of APTMS) or water (in case of APTES) containing 20 % of silane. Afterwards, APTMS and APTES substrates were rinsed with water several times to remove unbound silane and dried at room temperature and 120°C for 10 minutes, respectively. The silanized substrates were then immersed in the nanoparticle solutions for 24 h, rinsed with water to remove unbound nanoparticles and stored in water. For the mixed gold / silver surfaces, the silanized substrates were immersed in mixtures of gold and silver nanoparticle solutions with different amounts of gold and silver.

Characterization of plasmonic and nanostructure properties

UV/Vis spectra were recorded from all samples on a UV-Vis-NIR double-beam spectrophotometer (Jasco V-670) from 300 to 900 nm. For the measurements of the nanoparticles in solution quartz cells of 1 cm pathlength were used. The immobilized nanoparticles were measured directly on the glass by using a special sample holder.

The surfaces were imaged by scanning force microscopy (SFM) in intermittent contact mode under ambient conditions with a NanoWizard 2 (JPK Instruments AG, Germany) instrument, using silicon cantilevers (Olympus Corporation, Japan) with a typical resonant frequency of 70 kHz and a spring constant of about $2 \text{ N}\cdot\text{m}^{-1}$. Height, phase and amplitude images were recorded. The height of particles was measured using SPIP (Image Metrology A/S, Denmark).

The Scanning Electron Microscopy Images were obtained using a Hitachi S-4000 with a cold field emitter. The acceleration voltage was 15 kV. To enhance the conductivity of the sample a thin carbon film was evaporated.

Raman experiments and characterization regarding SERS performance

Normal Raman and SERS spectra were recorded using a Raman microscope (LabRamHR, Horiba, Jobin-Yvon, spectral resolution $\sim 2.5 \text{ cm}^{-1}$) with a 60x water immersion objective. A 632.8 nm HeNe-laser (1.5 micron spot diameter) was used for excitation of the Raman scattering. Typical spectra both for the Raman and the SERS experiment were collected in 1 second using a laser intensity on the sample of $6.7 \cdot 10^3 \text{ W}\cdot\text{cm}^{-2}$. For the investigation of the distribution of the enhancement factor, an area of $100 \times 100 \mu\text{m}$ on each substrate was mapped with a distance of $10 \mu\text{m}$ between each point in a rectangular grid.

Crystal violet (CV) concentration was $5 \cdot 10^{-6}$ M in the experiments with gold nanoparticles and $1 \cdot 10^{-6}$ M in the experiments with silver nanoparticles and in the mixtures of gold and silver nanoparticles. For determination of SERS enhancement factors (see next paragraph), normal Raman experiments were conducted using $5 \cdot 10^{-4}$ M CV in aqueous solution.

Enhancement factors (EF) were estimated by comparing intensities in the normal Raman spectrum (I_{RS}) and in the SERS spectrum (I_{SERS}) for the band at 1620 cm^{-1} of crystal violet, taking into account the number of molecules N_{SERS} and N_{RS} contributing to the SERS and Raman spectrum, respectively:

$$EF = \frac{I_{SERS} N_{RS}}{I_{RS} N_{SERS}} \quad (1)$$

Experiments on aqueous pollen extracts

Pollen extracts were obtained by covering a small amount of pollen from different species (*Populus nigra* ‘Italica’, *Secale cereale*, *Betula occidentalis*, *Artemisia tridentata*, all acquired from Sigma) with 100 μl deionized water (18,2 M Ω) for 10 minutes followed by centrifugation. For the SERS measurements with the gold nanoaggregates in solution, 2 μl of supernatant were mixed with 20 μl of the nanoaggregate solution. 100 spectra were taken from each sample. For the measurements on the gold nanoparticles immobilized with APTES, a drop of supernatant was placed on the nanoparticle layer. Spectra were recorded on an area of $100 \times 100 \mu\text{m}$ as described above. Afterwards, the spectra of each data set were averaged, and the coefficient of variation was determined. A 785 nm diode laser (intensity $6.5 \cdot 10^5 \text{ W} \cdot \text{cm}^{-2}$ in the measurements with the nanoparticles in solution, $1.3 \cdot 10^5 \text{ W} \cdot \text{cm}^{-2}$ in the measurements with the immobilized nanoparticles) was used for excitation.

Supporting Information References

- (1) Lee, P. C.; Meisel, D. *J. Phys. Chem.* **1982**, *86*, 3391.
- (2) Polte, J.; Herder, M.; Erler, R.; Rolf, S.; Fischer, A.; Würth, C.; Thünemann, A. F.; Kraehnert, R.; Emmerling, F. *Nanoscale* **2010**, *2*, 2463.
- (3) Joseph, V.; Matschulat, A.; Polte, J.; Rolf, S.; Emmerling, F.; Kneipp, J. *J. Raman Spec.* **2011**, *42*, 1736.
- (4) Blatchford, C. G.; Campbell, J. R.; Creighton, J. A. *Surface Science* **1982**, *120*, 435.
- (5) Shipway, A. N.; Lahav, M.; Gabai, R.; Willner, I. *Langmuir* **2000**, *16*, 8789.
- (6) Leopold, N.; Lendl, B. *J. Phys. Chem. B* **2003**, *107*, 5723.
- (7) Kneipp, J.; Li, X.; Sherwood, M.; Panne, U.; Kneipp, H.; Stockman, M. I.; Kneipp, K. *Anal. Chem.* **2008**, *80*, 4247.
- (8) Chumanov, G.; Sokolov, K.; Gregory, B. W.; Cotton, T. M. *J. Phys. Chem.* **1995**, *99*, 9466.
- (9) Grabar, K. C.; Freeman, R. G.; Hommer, M. B.; Natan, M. J. *Anal. Chem.* **1995**, *67*, 735.
- (10) Polwart, E.; Keir, R. L.; Davidson, C. M.; Smit, W. E.; Sadler, D. A. *Appl. Spec.* **2000**, *54*, 522.
- (11) Cant, N. E.; Critchley, K.; Zhang, H.-L.; Evans, S. D. *Thin Solid Films* **2003**, *426*, 31.